

D. REGENT<sup>1)</sup>, C. DELGOFFE<sup>1)</sup>,  
M. CLAUDON<sup>1)</sup>, D. THOMAS<sup>1)</sup>,  
J.F. CALAFAT<sup>1)</sup>, C. CHAULIEU<sup>1)</sup>  
and A. TREHEUX<sup>1)</sup>

# CT diagnosis of alveolar hydatid disease of the liver

<sup>1)</sup> Service Central de Radiologie, CHU Nancy-Brabois, Nancy, France.

Medicamundi, vol. 28, no. 2, 1983  
4522-984-53841/728

Alveolar hydatid disease of the liver (AHD) is a parasitosis with a pseudo-tumorous development which is, in general, relatively slow and insidious, but spontaneously fatal<sup>1</sup>. In addition to the anatomopathological data, an accurate diagnosis depends on immunological examinations of high specificity which are only carried out in a few very specialized centres. The results are usually only available after several weeks and their diagnostic value is not absolute (confusion between *Echinococcus granulosus* and *Echinococcus multilocularis*, together with false negatives, giving an overall sensitivity of the order of 95%)<sup>2</sup>. Despite the hope of effective treatment by medication (Flubendazole, Albendazole)<sup>12</sup>, only the total surgical removal of a still limited parasitic lesion can be considered as a complete cure of the patient. In view of the foregoing, methods for macroscopic visualization play an essential role in alveolar hydatid disease of the liver:

- for a positive diagnosis, which is difficult owing to the protean nature of the disease
- for determination of the extent of the lesions, the accuracy of which determines the possibility of surgical treatment.

Computed tomography has been shown to be the most effective examination method currently available. Using a series of 12 cases, and cases reported in the literature, it is possible to delineate the most significant features of the recently proposed 'CT syndrome of AHD'<sup>10</sup>.

## Anatomopathological and physiopathological background of hepatic AHD

Analysis of the CT signs of AHD of the liver requires an understanding of

**Summary.** A review of the anatomopathological and physiopathological background of alveolar hydatid disease of the liver, necessary for an understanding of the CT appearance of the disease, is followed by a report on twelve cases examined with the Philips Tomoscan 310.

The principal elements of the 'CT syndrome of alveolar hydatid disease of the liver' are enumerated and described, and the authors conclude that it is, above all, the combination of these elements which permits an accurate diagnosis to be made from the CT images in the vast majority of cases, and prevents the common confusion with primary or secondary malignant necrotic tumours of the liver.

the principal anatomopathological and physiopathological characteristics of the disease.

AHD results from the intrahepatic development in man of the larva or *hydatid* of *Echinococcus multilocularis* (a tapeworm which is a parasite in the intestine of the definitive host: fox, cat, dog, weasel, polecat, ferret... ). The development of this larva must be clearly differentiated from that of the *Echinococcus granulosus* larva, which causes the much more common and medically better known unilocular hydatid cysts.

Figure 1 shows the different characteristics of the unilocular hydatid cyst (*Echinococcus granulosus*) and the multilocular or 'alveolar' hydatid disease (*Echinococcus multilocularis*)<sup>3</sup>.

## Characteristics of alveolar hydatid disease

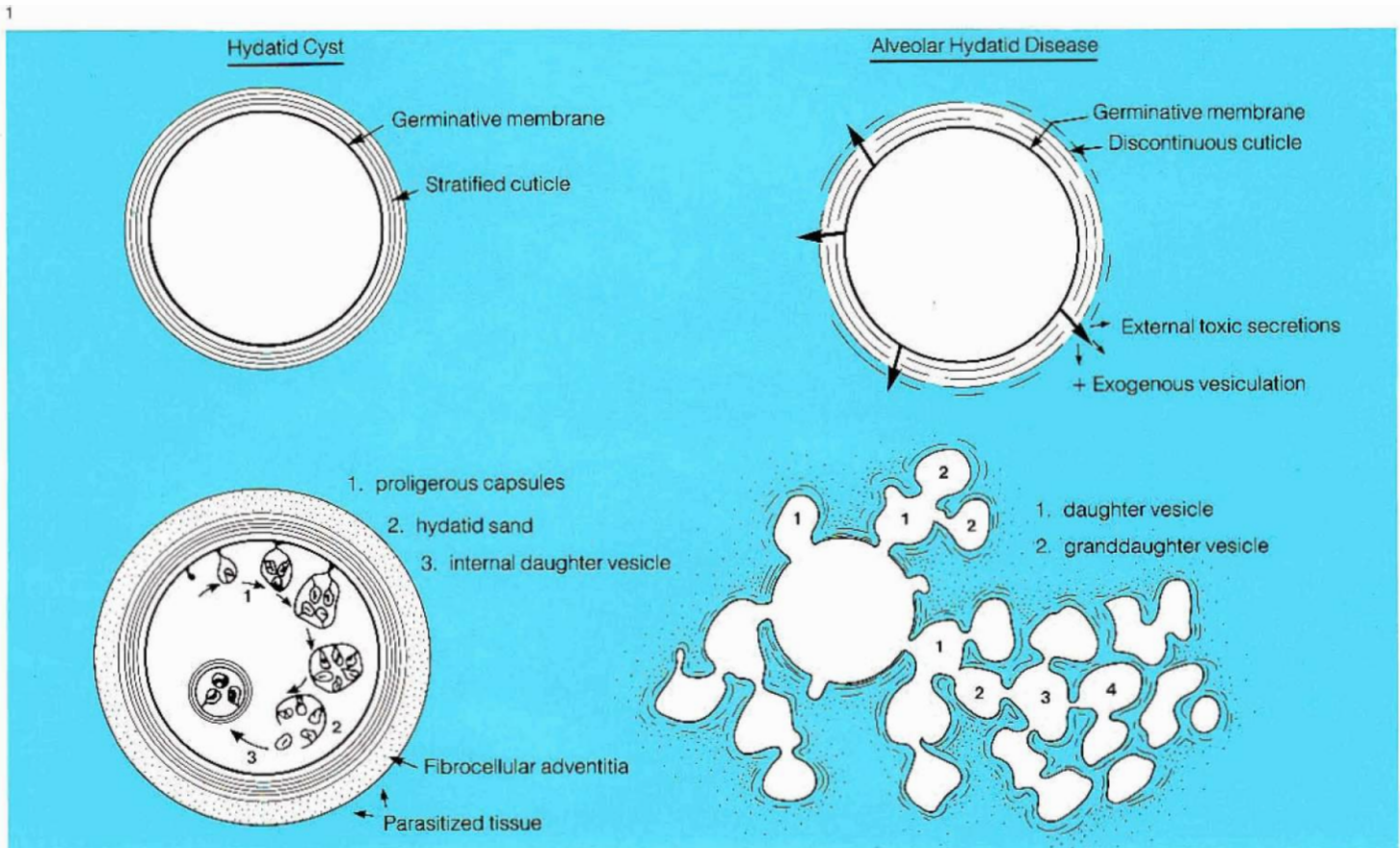
In alveolar hydatid disease the larva is surrounded by an external cuticle or stratified protective membrane which is of poor continuity, and does not ensure a clear separation between the parasite and the surrounding tissues. The external cuticle arises from the outer surface of the internal germinative or proliferous membrane, which is responsible for the growth of the lesion. This membrane produces

the germinative elements or scolices, which are the heads of the future adult worms and the form of infestation in the definitive host, and also produces a specific vesicular fluid which passes through the lacunae of the cuticle and has a necrotizing effect on the surrounding tissues.

The toxicity of the vesicular fluid and the dissolution of the continuity of the cuticle, together with a disorganized and energetic activity of the germinative membrane, account for the characteristic growth of the larval parasite by a *process of external vesiculation*, ending in an *infiltrating pseudotumorous formation* which produces fertile buds. These buds act as veritable pseudopodia, tending to infiltrate the portal tracts via the perivascular and peribiliary connective sheaths.

The host develops defence reactions in the form of *granulation tissue*, associated with *fibrosis* of which the intensity varies according to the aggressiveness of the parasitic larva. In man, who is an accidental intermediary host, the larval development is slow and the production of fibrous tissue is fairly limited; the inflammatory reaction is, however, quite marked and basically takes place from the inside to the outside: a histiocytic layer composed

Fig. 1. Comparative physiopathogenesis of lesions due to hydatid cyst (*E. granulosus*) and alveolar hydatid disease (*E. multilocularis*)<sup>1</sup>.



of a crown of epithelioid cells, followed by a granulomatous zone together with inflammatory infiltration and capillary hypervascularization. The granulomatous layer merges imperceptibly into a reticuline and collagenous fibroblastic encirclement reaction which infiltrates between the hepatic cords, separating them and reaching the portal tracts. These features are fundamentally different from those observed around the larvae of the *Echinococcus granulosus*, where the compressed and sclerosed tissue of the host forms a pseudo-capsule, the adventitia, at the periphery of the hydatid cyst, and the histiocytic reaction is only found in exceptional cases.

In AHD, the development of the parasitic mass ends in a *central*

*necrosis* leading to the formation of a cavity filled with a gelatinous magma, limited at the periphery by a dense tissue furrowed with numerous alveoli which give the disease its name. In the course of time, *foci of calcification* appear in the centre of the lesions, principally in the sclerotic zones, probably modified by ischaemic and infectious phenomena. The relatively slow growth of the parasitic process is accompanied by the development of a *marked compensatory hypertrophy of the healthy areas of the liver*, often partly responsible for the clinically perceived hepatomegaly. The extreme rapidity with which the liver develops such a compensatory hypertrophy after surgical excision is well known, but as far as the intrahepatic growth process

is concerned, it is observed mainly in the slow-growing, destructive lesions. The parasitic process within the hepatic mass develops: – mainly toward the *intrahepatic biliary ducts*, which are very often compressed (with dilatation upstream) but less often invaded; metastasis within the ducts is rare. The fibro-sclerotic *pericholangitis* frequently affects the region of the hepatic hilus, followed by the common bile ducts, explaining the icteric forms of the disease.

– toward the large intra- or extra-hepatic arterial and venous vascular branches, which are themselves surrounded by a fibrous perivasculitis, causing their stenosis and then obstruction. Specific parasitic invasions, the presence of adventitial

Fig. 2. Patients examined by the authors

| No. | Sex | Age | Duration of Development | Clinical Symptoms           | Surgical Interventions   |
|-----|-----|-----|-------------------------|-----------------------------|--|
| 1   | ♀   | 47  | 16 years                | hepatomegaly                | exploratory laparotomy (1967), cholecystectomy for cholelithiasis (1980)   |
| 2   | ♀   | 36  | 10 years                | icterus + HTP               | biliary derivation with omega loop (1972), ligation of oesophageal varices (1978), suture of bulbus ulcer (1980) |
| 3   | ♂   | 35  | 5 years                 | icterus + ascites (HTP)     | drainage of necrotic cavity in left hepatic lobe and internal biliary drainage of right lobe (1977)              |
| 4   | ♂   | 73  | 2.5 years               | hepatomegaly                | 0  |
| 5   | ♂   | 69  | 2 years                 | hepatomegaly                | discovery of AHD during cholecystectomy  |
| 6   | ♂   | 35  | 2 years                 | hepatomegaly                | exploratory laparotomy (1981) followed by left lobectomy (9/1981) and second exploratory laparotomy (7/1982)     |
| 7   | ♀   | 57  | 1 year                  | hepatomegaly                | exploratory laparotomy (1982)  |
| 8   | ♂   | 46  | 4 months                | hepatomegaly                | exploratory laparotomy (1982)  |
| 9   | ♂   | 67  | 3 months                | epigastric pain             | 0  |
| 10  | ♂   | 62  | 2 months                | hepatomegaly + icterus      | 0  |
| 11  | ♀   | 72  | 2 months                | hepatomegaly                | 0  |
| 12  | ♂   | 30  | 2 months                | pain in right hypochondrium | laparotomy for cholecystectomy   |

parasitic formations and the possibility of endoluminal penetration are also observed. This explains the venous complications of AHD of the liver which are most often manifested by hepatic block in the HTP portal network, but also by blockage in the cava-suprahepatic network (Budd-Chiari syndrome)<sup>18</sup>.

The extra-hepatic extent of the parasitic process can develop:

– progressively closer to the neighbouring organs, in particular the gallbladder and the pancreas, the lymph nodes of the porta hepatis and the lesser omentum, the diaphragm, the pleura and the right lung, the right kidney and right suprarenal gland, and the peritoneal cavity. It is sometimes difficult to differentiate these

affections from authentic haematogenic metastases<sup>4</sup>.

– via the blood vessels toward other organs (parasitic metastases). The brain and the lungs are the most common sites (approximately 10% of all cases)<sup>5</sup>

– localizations in bone are also encountered, particularly in the spine (2 recent cases in 64 observations). It is difficult to make a histological differential diagnosis between these lesions and the hydatid cysts of *Echinococcus granulosus*, as the latter frequently exhibit exogenous vesiculation in bone. Neurological complications are also common, particularly in the form of compression of the spinal cord. In our two cases, these were actually the indication of the disease.

### Case studies

*The patients.* CT examinations using a Philips Tomoscan 310 system were carried out in a group of 12 patients, consisting of 7 men and 5 women with ages ranging from 30 to 73 years, between 1 October 1981 and 1 April 1983 (Fig. 2).

Seven patients had been followed for several years (one for 16 years, 3 for more than 5 years) and treated with Flubendazole since 1979, replaced by Albendazole in 1982. Some of them had undergone various palliative surgical procedures: biliary drainage (2), external drainage of a necrotic cavity (1), haemostasis for digestive tract haemorrhages caused by rupture of oesophageal varices (1) or by duodenal ulcer (1) viz. four surgical

interventions in two patients (numbers 2 and 3). One patient, followed in another medical centre, had undergone a left lobectomy and two exploratory laparotomies for biopsy (number 6).

– In the last five patients, the disease has been discovered in the last eighteen months, the CT examination being part of the initial assessment of the extent of the disease. These patients have also been treated by medication. No attempt at curative surgical excision has been made in any of the patients.

#### Method

The CT examinations were all carried out on the Philips Tomoscan 310 system (acquisition time 4.5 s, field of view 32 cm, slice thickness 9 mm, increment  $1.5 \times 9 = 13.5$  mm, reconstruction matrix  $256 \times 256$ , viewing matrix  $512 \times 512$ ).

All examinations, with one exception, were standard investigations after injection of a contrast medium bolus (60 ml Telebrix 38<sup>®</sup>) followed by a perfusion of 100 to 160 ml of the same material.

Recent examinations (since December 1982) have benefitted from the sequential, dynamic examination mode with image reconstruction in different time sequences, particularly useful for studying the suprahepatic portal and venous vascular complications.

All patients were given an ultrasound examination, some days before the CT examination, which was performed by the same operator. Real-time studies with sector scan (Sonel 400 CGR) and contact scan studies with a digital unit (Philips Sono Diagnost B52) were both carried out.

#### Results (Fig. 3)

##### *CT morphology of hepatic AHD.*

Detection of hepatomegaly has only minor specific significance. It is

associated with the development of parasitic lesions and/or compensatory hypertrophy of the healthy segments. It can be total or segmentary and is found in all cases.

The topography and the dimensions of the affected areas are more interesting. The parasitic infection was multifocal in 4 of the 12 cases studied. In three cases the lesion consisted of a principal focus and secondary nodular localizations. In all other cases the lesion had a single focus. The largest dimension of the affected area within the plane of the slices was equal to or greater than 10 cm in 7 of the 12 cases, and in particular in the last 5 cases observed.

The left lobe of the liver was affected in 8 out of 12 cases, but the lesion was never limited to this single lobe. The right lobe of the liver was affected in 10 of the 12 cases (in 4 of which the lesion was strictly limited to this lobe); the hilar region was involved in five cases.


With respect to the attenuation values, the most salient facts are the generally hypodense nature of the lesions (10 of the cases), less marked in the retractile affections, and their heterogeneous character (Fig. 4). This last point is the result of the formation of lacunar images within the mass (necrosis) as well as in the periphery of the principal lesion (large alveoli). It is responsible for the 'scalloping' contours before and after contrast medium injection. These images are observed in all cases. The measurements of the attenuation values show variations from  $-26$  to  $479$  H.

Calcifications were found in 11 of the 12 cases. Taken in combination with the preceding observations, these represent a feature of great importance (Figs. 5 to 8):

– in 9 cases, they had the appearance of a fairly large mass of disparate

Fig. 3. Analysis of CT images of the liver

| No. | Number of lesions | Site                          | Size in cm |
|-----|-------------------|-------------------------------|------------|
| 1   | 2                 | II + III<br>V + VI            | 7,5<br>6   |
| 2   | 1                 | V + VI<br>IV + III            | 15         |
| 3   | 2                 | II + III + IV<br>V + VI + VII | 8<br>16    |
| 4   | 1                 | II + III + IV +<br>VI + VII   | 18         |
| 5   | >1                | VIII<br>III(?)                | 9<br>2     |
| 6   | 2                 | II + III<br>IV + V + VI + VII | 15         |
| 7   | 1                 | VI                            | 6          |
| 8   | 1                 | VI                            | 15         |
| 9   | 1                 | IV + II + III                 | 12         |
| 10  | 1                 | II + III + IV                 | 15         |
| 11  | 1                 | V + VI                        | 11         |
| 12  | 1                 | V + VI                        | 13,5       |

| Heterogeneous hypodense mass | WITHOUT CONTRAST MEDIUM |  |            | WITH CONTRAST MEDIUM         |                                     |                     | Compensatory hypertrophy   |
|------------------------------|-------------------------|--|------------|------------------------------|-------------------------------------|---------------------|--|
|                              | Attenuation values      | Calcifications                         | Retraction | Improved contour delineation | Peripheral lacunar images (alveoli) | Perilesional border |  |
| ++                           | 30-94                   | micronodular                           | +++        | +++                          | ++                                  | 0                   | ++   |
| +                            | 3-267                   | macronodular + plaques                 | +++        | +++                          | +++                                 | 0                   | right lobe segment VIII  |
| +                            | 5-296                   | micronodular<br>macronodular + plaques | +++        | ++                           | 0                                   | 0                   | +++<br>left lobe   |
| +                            | 6-131                   | plaques                                | +++        | +                            | ++                                  | 0                   |  |
| ++                           | 2-126                   | 0                                      | 0          | ++                           | 0                                   | ++                  | —  |
| +++                          | 26-100                  | nodular + perilesional border          | +          | +++                          | 0                                   | 0                   | ++ left lobe + tip of right lobe   |
| +++                          | 13-167                  | in plaques                             | +          | ++                           | +++                                 | 0                   | caudate lobe   |
| 0                            | >200                    | nodular                                | +          | —                            | —                                   | —                   | + right lobe   |
| +++                          | 6-180                   | nodular                                | +          | +++                          | +++                                 | 0                   |  |
| +++                          | 25-35                   | 0                                      | +          | +++                          | 0                                   | ±                   |  |
| +++                          | -5-248                  | nodular + peripheral border            | +++        | +++                          | +++                                 | 0                   | +++ left lobe  |
| ++                           | 0-479                   | nodular in plaques                     | ++         | ++                           | +++                                 | 0                   | + right lobe   |
| ++                           | 29-100                  | micronodular in cloudy clusters        | ++         | +++                          | ++                                  | 0                   | +++ caudate lobe   |
| +++                          | 30-110                  | nodular heterogeneous                  | ++         | +++                          | +++                                 | 0                   | ++ left lobe  |
| +++                          | -20-190                 | nodular                                | ++         | +++                          | ++                                  | 0                   | ++ VII, VIII left lobe   |

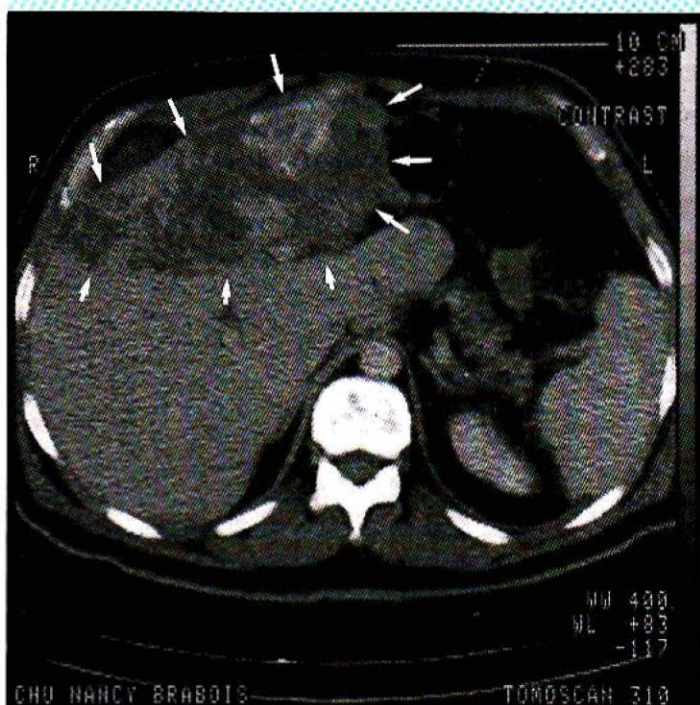
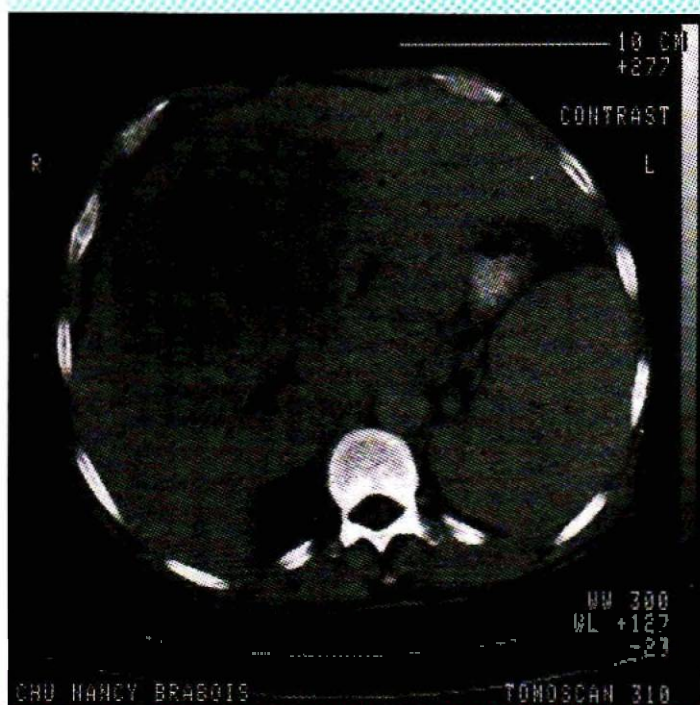
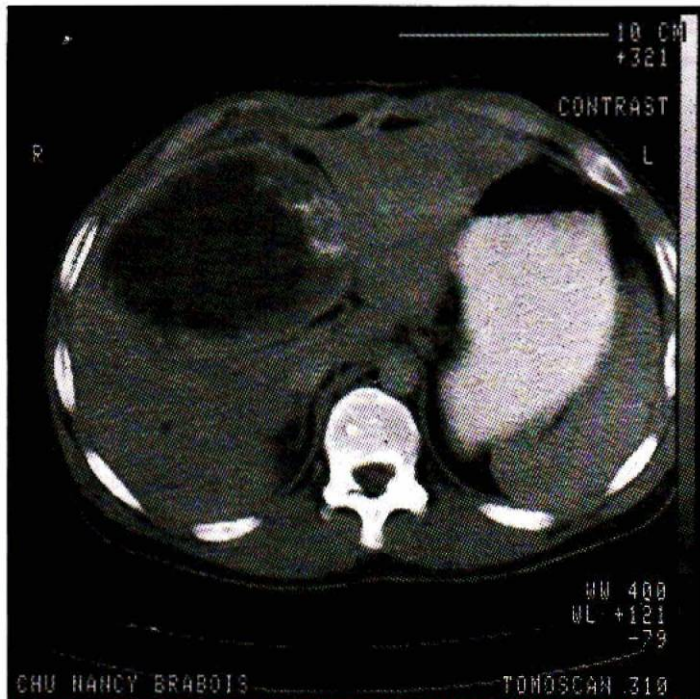


**Fig. 4. Structural heterogeneity characterized by the wide range of the attenuation values in three cases of AHD.**

- a. 'Fluid' form with a thick calcified wall in the internal region (case 12).
- b. 'Necrotic' form with poorly-defined contours, even after contrast medium injection. HTP by hepatic blockage (splenomegaly) (case 4).
- c. 'Infiltrating' form of a retractile nature (large arrows on the anterior and internal edges). Scattered micronodular calcifications (case 10).

**Fig. 5. Nodular calcifications.**

- a. Associated with a general retraction of the left part of the liver (segments IV, III, II) (case 9).
- b. Associated with a retraction of segments V and VI (irregular polycyclic contours, arrowed). Dilatation of intrahepatic bile ducts in the left part of the liver. HTP (Splenomegaly) (case 2).

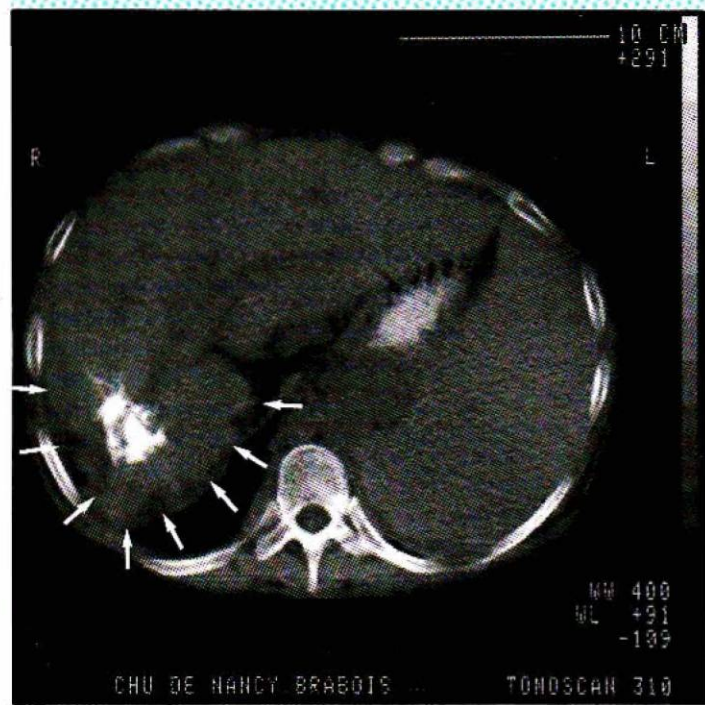
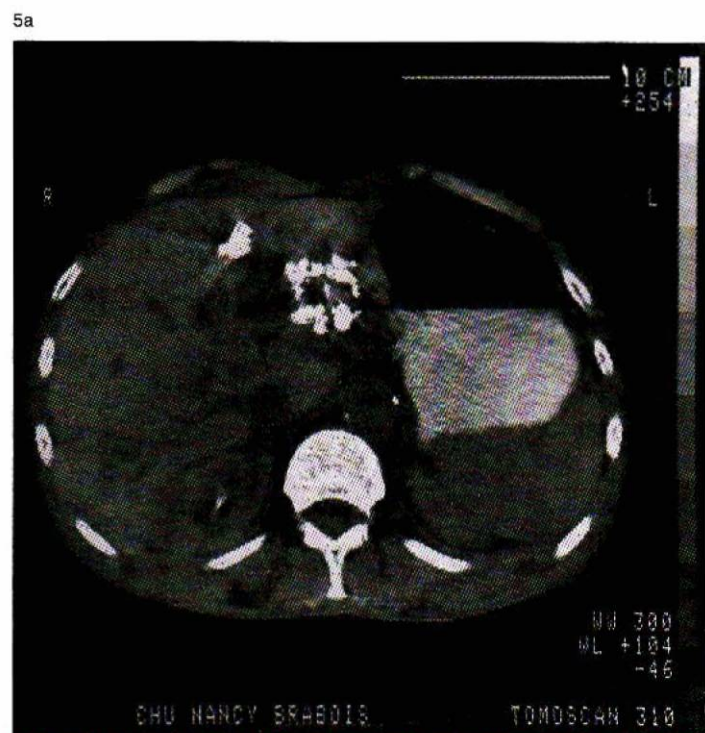
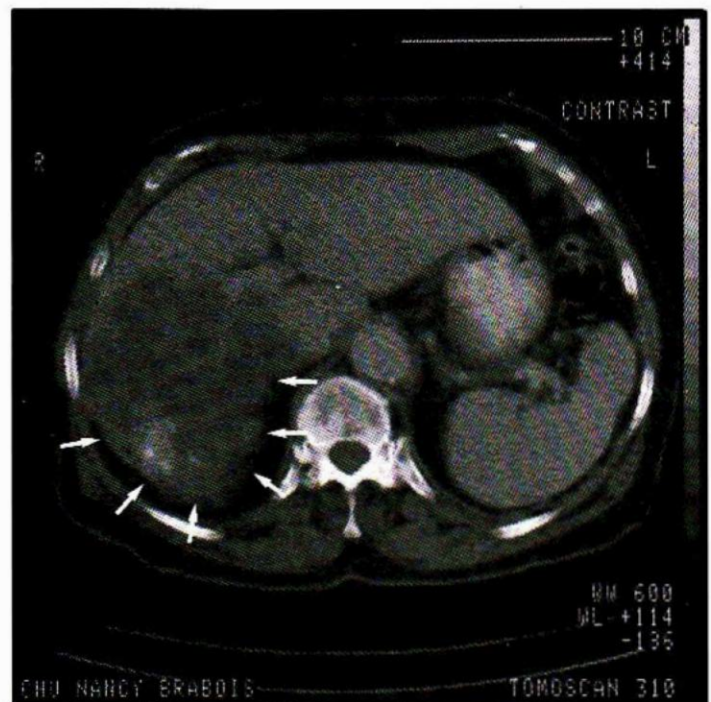
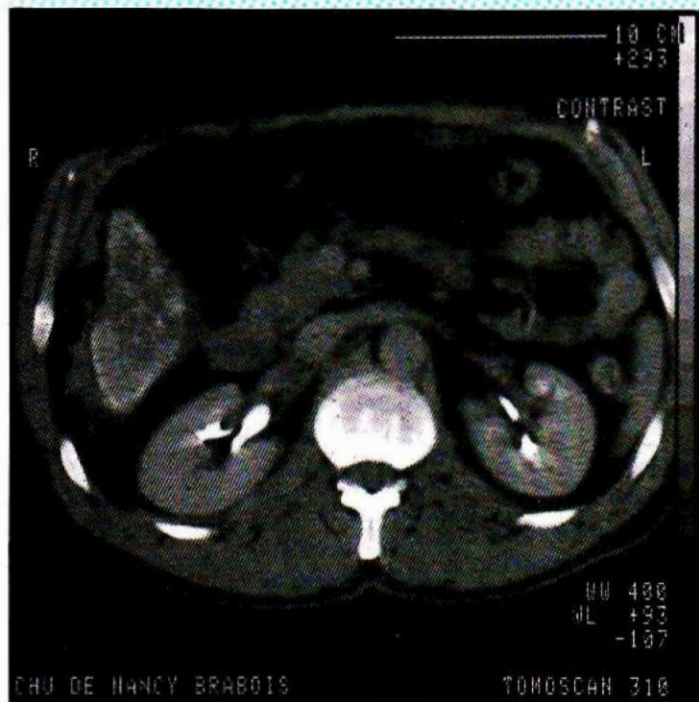
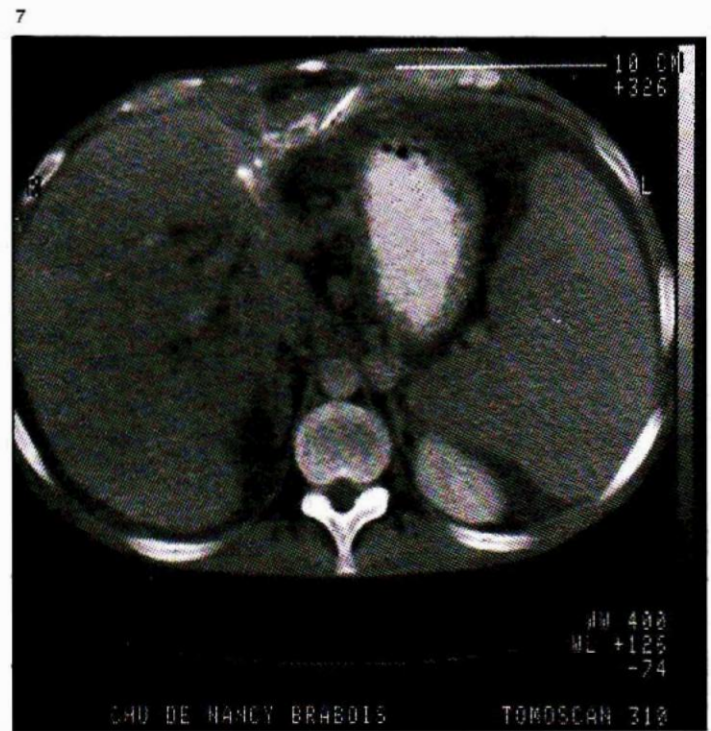
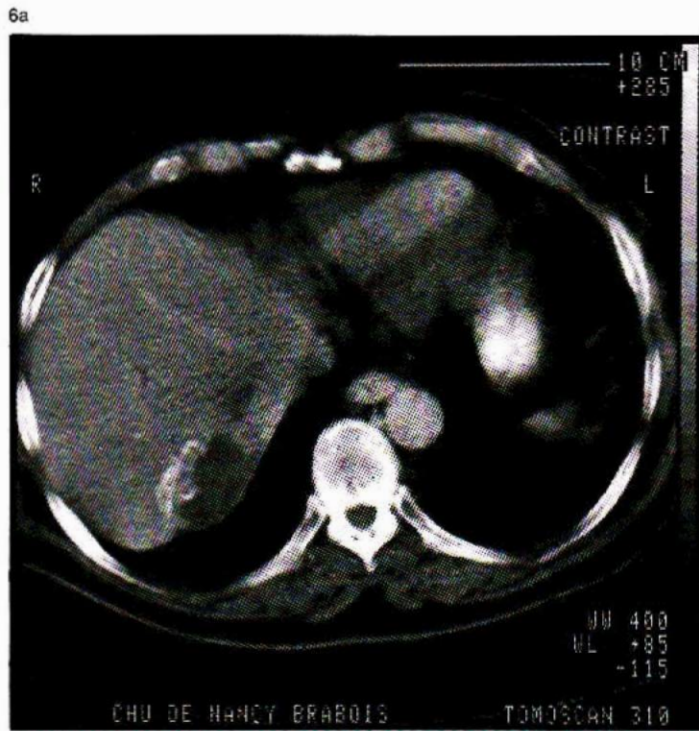


Fig. 6. Calcifications in plaques.

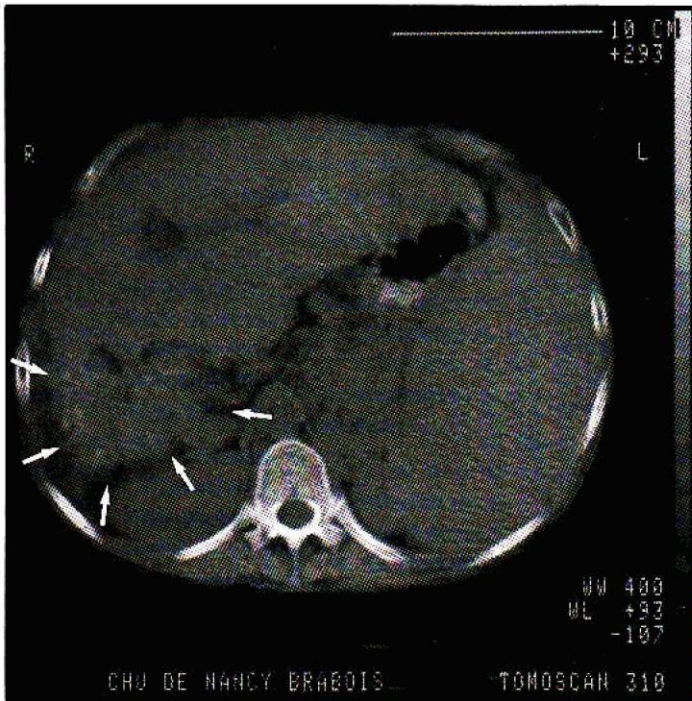
- a. Thick localized plaque at the periphery of a fluid lesion (case 5).
- b. Nodular calcifications, distributed in plaques in the capsular region, with retraction (case 8).

Fig. 7. Major retraction of the left part of the liver after external surgical drainage of a cavity. Calcifications in plaques (case 3).

Fig. 8. Generally hypodense heterogeneous mass in segments V and VI. Heterogeneous micronodular calcifications with retraction in the capsular region (case 11).



9a



9b

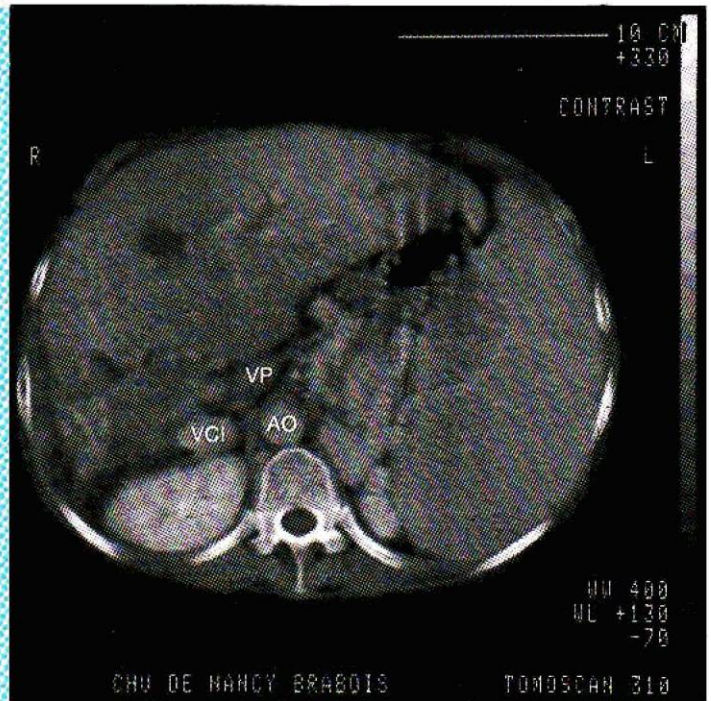


Fig. 9. Retraction and nodular calcifications of segments V and VI. HTP by hepatic block (case 2).

a. Before contrast medium injection.

b. After contrast medium bolus injection.

Fig. 10. Very significant segmentary retraction opposite a necrotic lesion developing into a fibrous regression under treatment first by Flubendazole® and then by Albendazole®. Note also the peripheral lacunar images (alveoli), clearly visible after contrast medium injection (outline arrows).



10



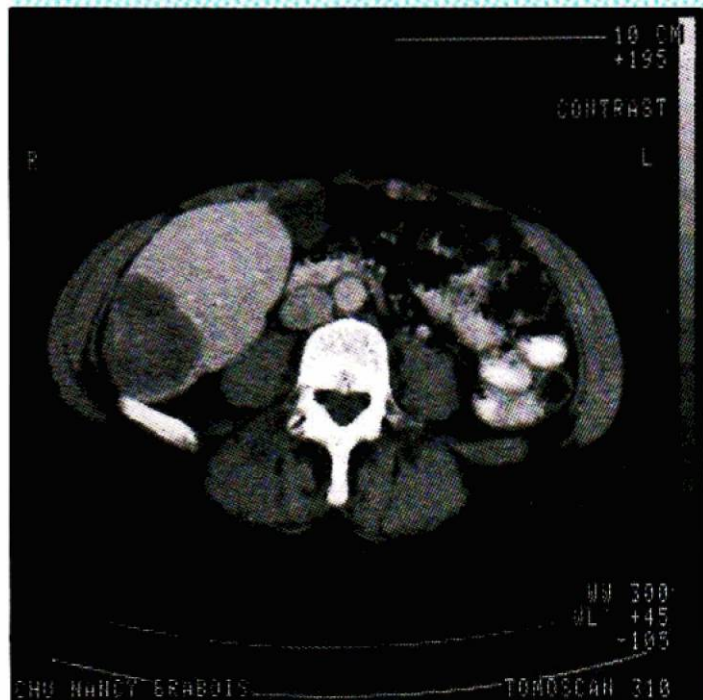
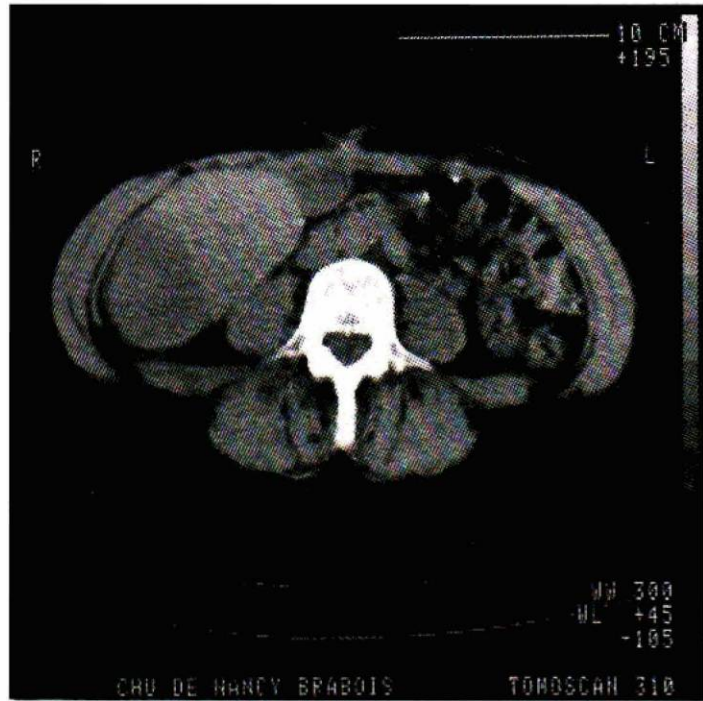
**Fig. 11.** The enhancement of the healthy parenchyma after contrast medium injection allows clear delineation of the lesion (case 7).

a. Before contrast medium injection.

b. After contrast medium injection.

*N.B.* This is the only non-calcified lesion in the study.

11a



11b

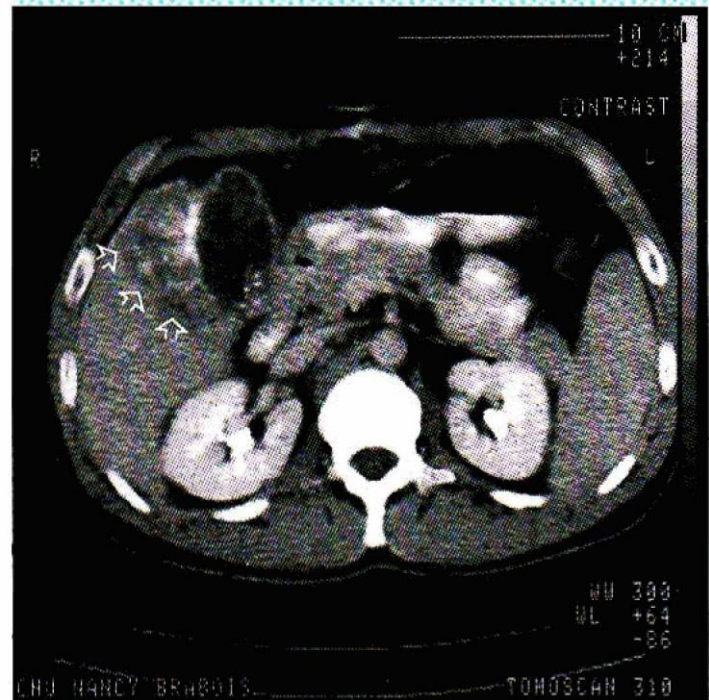
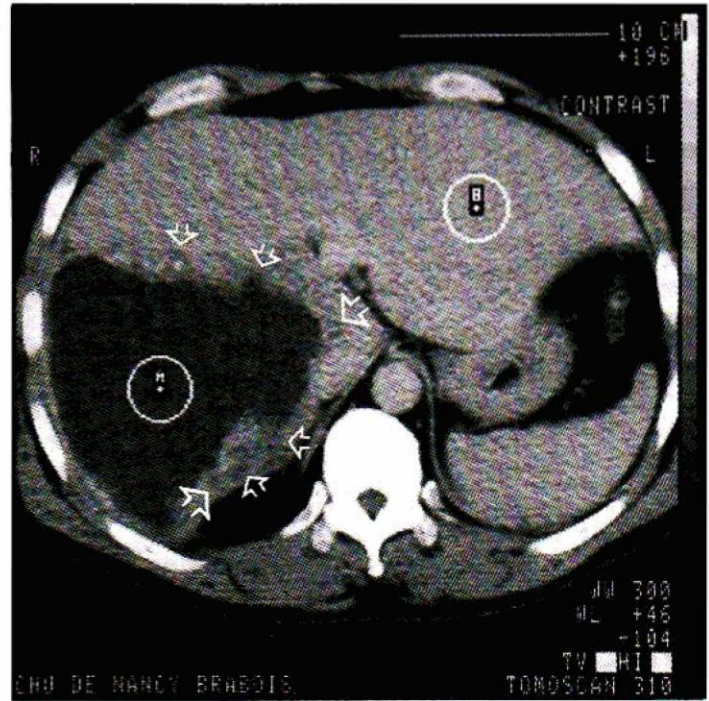
**Fig. 12.** The injection of contrast medium clearly shows the lesional contours and permits, in particular, visualization of the peripheral lacunar images (alveoli).

a. Essentially fluid lesion of segments V and VI.

Note the small micronodular calcifications (case 8).

b. 'Mixed' necrotic and calcified lesion (case 11).

12a



12b

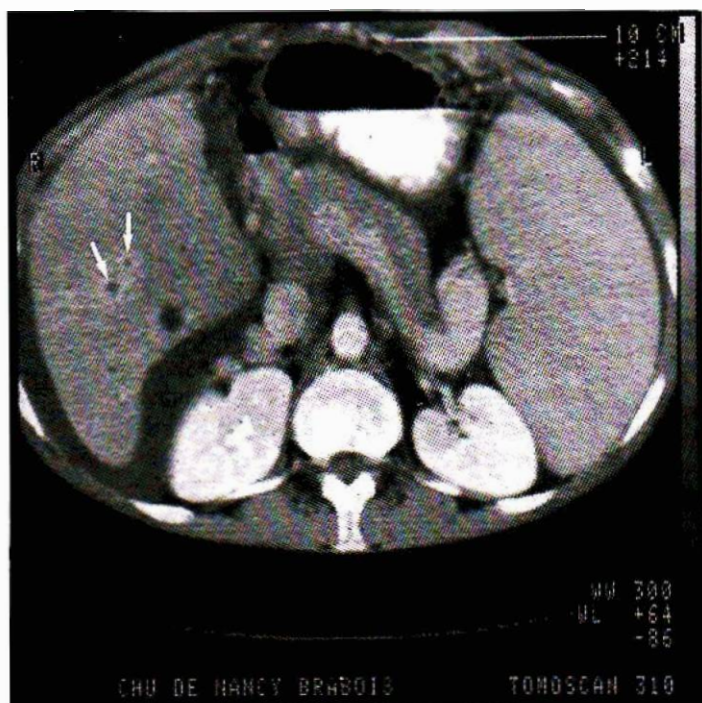


Fig. 13. Slight enhancement of perilesional border in the nodular lesions of the right lobe of the liver following injection of contrast medium (case 3).

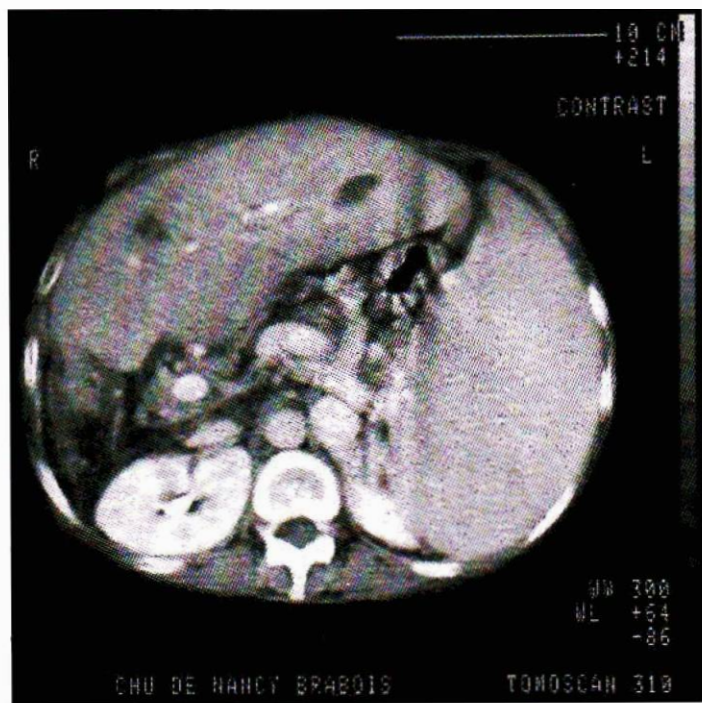


Fig. 15. HTP by hepatic block with voluminous venous vessels derived from the perigastro-oesophageal and porta-systemic shunts (case 2).

Fig. 14. Analysis of complications of AHD in the vascular and biliary systems in computed tomography.

| No | Portal network  | VASCULAR COMPLICATIONS                          |   | BILIARY COMPLICATIONS |                 |
|----|---|---|---|-----------------------|-----------------|
|    |   | suprahepatic veins                              | Inferior vena cava (IVC)                                    | Hilar lesions         | Dilatation IHBD |
| 1  | 0   | Total length of left suprahepatic vein stenosed | 0   | 0                     | 0               |
| 2  | Major HTP + porta-cava venous derivations                       | Middle and right suprahepatic veins not visible | 0   | ++                    | +++ left lobe   |
| 3  | Major HTP + porta-cava derivations + ascites + portal cavernoma | Suprahepatic veins not visible                  | IVC dilated in its sub-hepatic segment affected by the mass | +++                   | ++ right lobe   |
| 4  | HTP splenomegaly + derived vessels                              | Supra hepatic veins not visible                 | IVC not clearly identifiable, affected by the mass          | +                     | ++ left lobe    |
| 5  | 0   | 0   | 0   | 0                     | 0               |
| 6  | 0   | 0   | In contact with IVC which is compressed                     | 0                     | 0               |
| 7  | 0   | 0   | 0   | 0                     | 0               |
| 8  | 0   | Suprahepatic veins not visible                  | In contact with IVC   | 0                     | 0               |
| 9  | 0   | Displaced suprahepatic vein                     | 0   | 0                     | + right lobe    |
| 10 | 0   | Suprahepatic veins not visible                  | 0   | 0                     | + left lobe     |
| 11 | 0   | Suprahepatic veins not seen                     | In contact with IVC   | In contact            | 0               |
| 12 | 0   | 0   | In contact with left and middle suprahepatic vein           | In contact            | 0               |

nodules, heterogeneously dispersed at the middle or periphery of the affected areas

- in 5 cases, they appeared as arciform calcified plaques at the periphery of the fluid zones
- in 9 cases, they were associated with retraction images of the parenchyma
- in 4 cases, they appeared as a scattering of micronodules, in one case distributed heterogeneously within the mass and, in another case, forming a perilesional border.

In five out of eleven cases, these calcifications were missed in the first evaluation of an abdominal plain film (without preparation). On further study, they could only be guessed at in another three cases. In the remaining two cases, the calcifications were only visible in the CT images.

The retractile appearance of the lesions seems very significant, as it was found in all 12 cases. It is

characterized by a reduction in the volume of all or part of the affected hepatic segment, the contours of which retract and assume a particular and very typical polycyclical appearance (Figs. 9, 10). It is found in varying degrees, depending on the location. It was very obvious in 4 cases, fairly clear in 4 others and less clear in the remaining four. Because of the quality of the images, CT scanning permits careful analysis of the hepatic contours, perfectly demonstrating the retraction images, which are of great diagnostic value, but appear to be much more difficult to detect in an ultrasound examination.

An examination with contrast medium follows the basic CT examination as a matter of routine. There is a considerable improvement in the delineation of the lesion, as its poor vascularization leads to an absence of enhancement at the site of the lesion,

*Fig. 16. Effect of AHD on the cava-suprahepatic venous system.*

*a. Atrophic form of AHD of the left lobe studded with micronodular calcifications. The left suprahepatic vein appears contracted along its entire irregular length, while its middle and right counterparts are well visualized (case 1).*

*b. Voluminous lesion of the right part of the liver with compensatory hypertrophy of the caudate lobe. The inferior vena cava (arrow) is compressed by the parenchyma, which is in turn displaced by the lesion, but remains patent.*

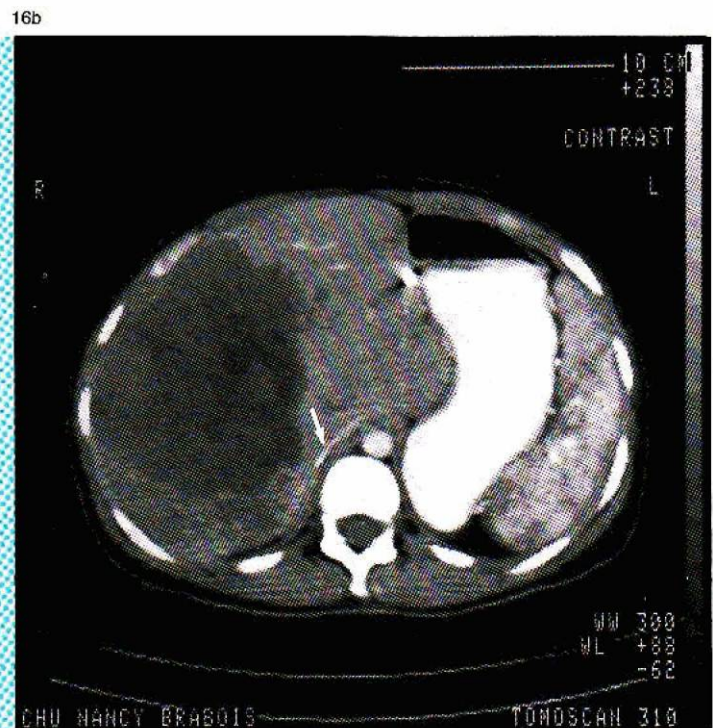
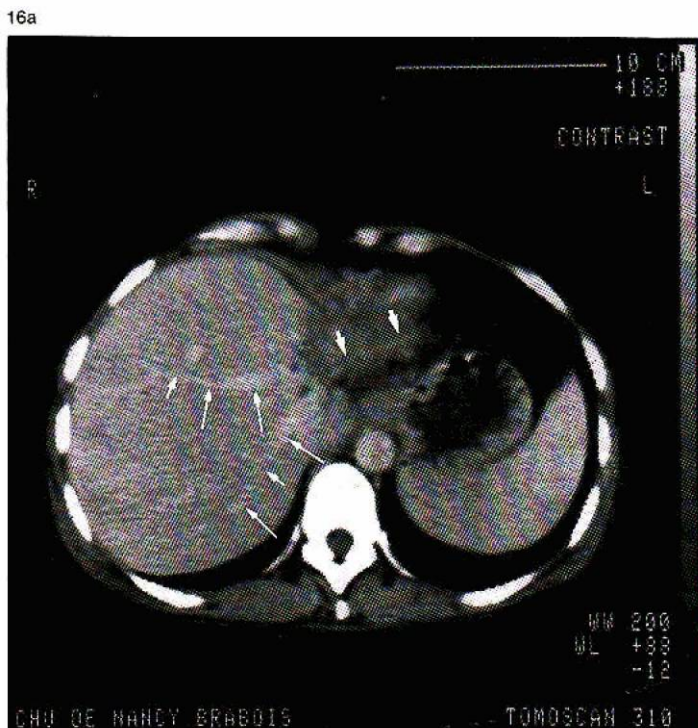
and it provides a clear contrast with healthy parenchyma (Fig. 11)

Consequently the analysis of lesional contours is facilitated and it is only then that it is possible to identify the irregular polycyclical appearance (12 out of 12 cases) and the frequent presence of lacunar lesions (large alveoli) around the principal lesion (9 out of 12 cases) (Fig. 12).

The rapid sequential mode study, after injection of a first contrast medium bolus, permits the visualization of only a very small border of perilesional enhancement in two cases (Fig. 13). The infrequency and relative moderation of this phenomenon represent an important, distinctive element which eliminates the possibility of an abscessed lesion or a necrotic hypervascularized tumour.

*CT evaluation of complications affecting the vascular system (Fig. 14).*

Complications of hepatic infection affecting the portal circulation were



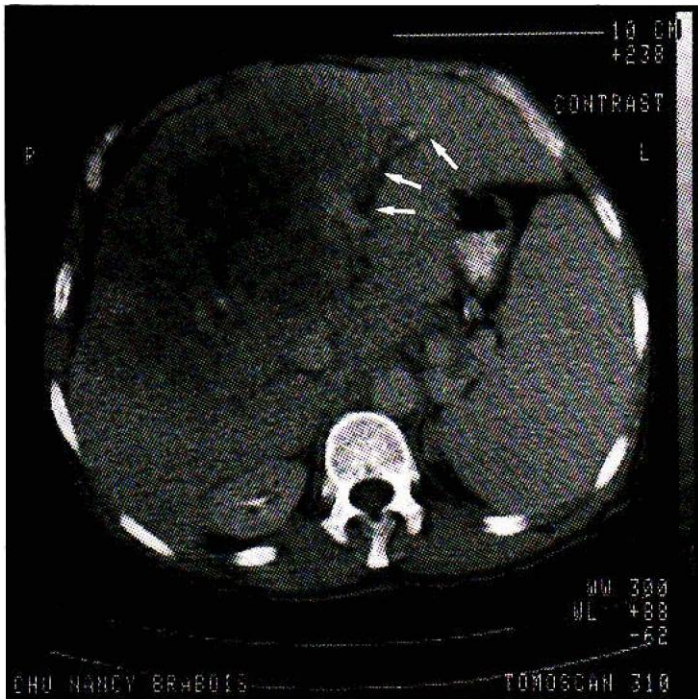


*Fig. 17. Segmentary dilatation of the intra-hepatic bile ducts of the left lobe, related to hilar extension of a voluminous lesion of the right part of the liver. HTP by hepatic block (case 4).*

observed in three cases, involving splenomegaly and major dilatation of the splenic vein (Fig. 15). By employing the rapid sequential mode it is possible to determine the condition of the portal vein and the derivative vessels in the case of hepatic or prehepatic block.

Complications of hepatic lesions affecting the suprahepatic veins and/or the inferior vena cava can also be suspected (4 cases) when the lesion is adjacent to, displaces or obliterates the image of these vascular structures (Fig. 16) but it should be recognized that an accurate diagnosis is very difficult and will require a conventional angiographic examination.

**CT evaluation of complications affecting the biliary system.** The exact evaluation of biliary complications from CT slices is often difficult. There are some obvious cases (Fig. 17) in which images of dilatation of the intrahepatic bile ducts can be observed

in an icteric patient where the lesion clearly affects the hilar region. However, the clear visualization of a moderate, segmentary dilatation of the intrahepatic bile ducts is generally much more difficult. In order to differentiate between the vascular and biliary structures at the level of the portal tracts, contrast medium injection is required.

Lesions of this nature were only observed in the CT images in two cases. Ultrasound examination has not been more effective, as visualization of the intrahepatic biliary ducts is often impossible due to major changes in the liver.

#### **Observations on the diagnostic value of CT images**

CT scanning is an extremely effective technique for the morphological diagnosis of alveolar hydatid disease of the liver. The principal elements of the 'CT syndrome of AHD' are as follows:

- The detection of a mass, which is usually voluminous and generally hypodense in comparison with the hepatic parenchyma, with poorly defined irregular borders. The mass has a very heterogeneous appearance, with attenuation values ranging from those of the 'fluid' zones to the density of calcifications.

- The calcifications form a significant element which, in view of their frequent occurrence, is of great value. They can be situated either in the lesion or at the periphery of the mass, and assume the most diverse morphological appearances. They are sometimes missed during a rapid examination of plain films of the abdomen. They have no correlation with the extent of the lesion<sup>3</sup>.

- The retraction of the lesions is a major characteristic, which appears to be fairly specific as it is not reported in CT studies of expansive tumorous processes in the liver<sup>1, 11, 15</sup>. However, as the segmentary retracted lesions of

AHD have a mean density close to that of the hepatic parenchyma, they are best studied by examination of the liver contours, with their characteristic 'notched' polycyclical appearance, and by detection of the frequently associated microcalcifications. This means that a CT system is required which will provide the highest level of spatial resolution and contrast discrimination, and makes it essential to have facilities on the operator's console for careful study of the images by selecting the appropriate window and mean density settings for precisely determining the hepatic contours.

– The injection of contrast medium increases the attenuation values of the healthy parenchyma, providing better delineation of the lesions and a clearer visualization of their internal structure, particularly for determining the heterogeneous character of the mass and the frequent presence of lacunae or peripheral alveoli.

– Finally, the compensatory hypertrophy of the healthy hepatic areas is also an important pathognomonic criterion, indicative of the slow development of the disease.

In general, these characteristics match those described in the literature.

However, we have not found segmentary dilatation of the intrahepatic bile ducts with any degree of frequency, although this element has been described as significant by Haertel<sup>8</sup> and later by Lassègue<sup>10</sup>. Similarly, we have not found hilar affection as frequently as quoted<sup>10</sup>. This could be explained by the fact that the majority of the patients in our study, with the exception of the oldest, developed lesions which, although extensive, were fairly peripheral and were not accompanied by jaundice or any biological syndrome of cholestasis.

The principal problems of differential diagnosis are represented by the necrotic forms of primary or secondary tumours of the liver, on one hand, and infectious, abscessed lesions on the other hand.

Necrotic malignant tumours of the liver, like certain benign tumours, are generally heterogeneously hypodense and can calcify spontaneously or as a result of the treatment which is applied to them. Of 230 hepatic focal lesions studied by computed tomography by Scatarige et al.<sup>14</sup>, 28 (12.2%) are the site of calcifications of which 9 out of 59 (15.3%) are malignant hepatomas, 15 out of 82 (18.3%) are metastases of colonic cancer, 2 out of 71 (2.8%) are metastases of non-colonic cancer and 2 out of 18 (11%) are benign hepatic masses (adenomas).

The literature notes calcified hepatic metastases essentially in primitive mucosecreting colonic lesions but also, less commonly, in pseudomucinous cystadenocarcinomas of the ovary, gastric adenocarcinomas, endocrine cancers of the pancreas, adenocarcinomas of the kidney and breast or melanomas<sup>11</sup>. There are also reports of cases of calcified metastases of the liver in neuroblastomas, pleural mesotheliomas, osteosarcomas, leiomyosarcomas, carcinoid tumours, cholangiosarcomas, myelomas and lymphomas. In all studies, the frequency of tumorous calcifications did not exceed 25% of cases of primary tumours of the liver and 18.3% of cases of hepatic metastases of colonic cancers (this last figure is for a group of patients presenting massive lesions, treated by chemo- and radiotherapy)<sup>14</sup>. There is no specificity of the morphological type of the calcifications, which seem to be the result of haemorrhagic or, especially, necrotic phenomena within the tumor masses.

Hepatic abscesses can also calcify and show features resembling AHD in computed tomography. Haertel<sup>8</sup> and Scherer<sup>15</sup> think that the differential diagnosis is impossible from the observed images alone. The presence of air within the lesion is not a decisive argument, as it can be observed in cases of biliary fistula in AHD. A valuable diagnostic element in favour of an abscess is the observation of 'annular' peripheral contrast, but it is not always present or specific<sup>16</sup>. Tuberculosis should be included among the infectious hepatic lesions which are capable of posing serious problems for a differential diagnosis, as it can cause retraction and calcification phenomena, as well as dilatation of the intrahepatic bile ducts when there is, for example, a compression of the choledochus by adenopathies of the pedicle. From the foregoing it can be concluded that those elements which, in the CT images alone, are indicative of AHD are as follows:

- the frequency of calcifications (they are found in more than 90% of cases of AHD)
- features of retraction in the pseudotumorous zones
- the presence of 'alveolar' lacunar images on the periphery of the mass(es)
- the absence, or moderation, of enhancement of the perilesional border.

It is essentially the combination of these characteristics which permits the diagnosis of AHD and which avoids 'easy' confusion with tumorous pathology.

*Comparison of ultrasound and CT.* A comparison of ultrasound and CT results comes out very much in favour of the latter technique. Apart from ease of operation and low cost, the

advantages of ultrasound in terms of information quality are the visualization of necrotic masses in the study of the intra- as well as extra-hepatic biliary ducts, and in studies of the suprahepatic and inferior cava vascular structures<sup>3</sup>. However, there is some disadvantage in the use of ultrasound in visualizing the condition of the parenchyma, when calcifications reflect the ultrasound waves or when the lesion largely absorbs sound waves. The exact form of the liver contours is often poorly shown, the difficulties being exacerbated when the hepatic morphology has been modified by anterior interventions.

If ultrasound constitutes the ideal means detecting infections by the identification of a hepatic focal mass as well as for the evaluation of its effect on the biliary and venous systems, its lack of precision and reproducibility practically denies it any role in the exact determination of the intra-parenchymatous extent of the parasitic process. Ultrasound and computed tomography are, therefore, two complementary morphological approaches in the assessment of AHD of the liver and it is only possible to subscribe to the opinion of Lassègue<sup>10</sup> who recommends:

— middle-term monitoring (1 examination every 6 months) by ultrasound performed by doctors conversant with the problems posed by this affection

— annual evaluation of the hepatic mass by computed tomography which, by the accuracy of its parameters and the precision of its images, permits only objective reproducible and storable comparison of the findings.

**Angiography.** The place of angiography in the positive diagnosis of AHD is, at the present time, considerably reduced, despite the precision of the images that it

provides<sup>2,3</sup>. This technique must now be reserved for the pre-operative evaluation of portal and cava-suprahepatic vascular structures.

### Conclusion

Morphological diagnosis of AHD of the liver is possible in the vast majority of cases, based on careful analysis of the CT images. These images, made after the injection of contrast medium, show a principal hypodense heterogeneous lesion with irregular contours that are practically always calcified and very often retracted. The internal structure frequently shows multiple lacunae at the periphery.

Confirmation of the diagnosis can, as a rule, be obtained non-sanguinously from the immunological data. It is to be hoped, however, that the development of abdominal echography will make it possible to detect the disease at an increasingly earlier stage, in order to provide a real possibility of truly curative surgical removal.

### Bibliography

1. Baert, A.L., Wackenheim, A. and Jeanmart, J., *Abdominal Computer Tomography*. Springer Verlag Berlin (1980).
2. Bessot, M., Treheux, A., Gaucher, P., Regent, D., Richaume, B. and Fays, J., *L'Artériographie de l'Echinococcose Alvéolaire Tyrolo-Bavaroise*, *Med. Chir. Dig.* 4: 39-44 (1975).
3. Claudon, M., *Place Actuelle des Méthodes d'Imagerie dans le Diagnostic et la Surveillance de l'Echinococcose Alvéolaire*. A propos de 62 Observations Recueillies en Lorraine, Thèse médecine Nancy, (1983).
4. Gabriel, A., *L'Echinococcose Alvéolaire du Foie en Lorraine*. A propos de 44 observations, Thèse méd. Nancy, (1976).
5. Gabriel, A., *Les Métastases Pulmonaires de l'Echinococcose Alvéolaire du Foie*. A propos de 2 Observations, *Memoire CES mal. App. digestif*, (1978).
6. Grabbe, E., Kern, P. and Heller, M., *Human Echinococcosis: Diagnostic Value of Computed Tomography*, *Tropenmed. Parasit.* 32: 35-38 (1981).

7. Grosdidier, J., Richaume, B. and Boissel, P., *Traitement Chirurgical de l'Echinococcose Alvéolaire*, *Med. Chir. Dig.* 4: 45-49 (1975).
8. Haertel, M., Fretz, C. and Fuchs, W.A., *Zur Computer Tomographischen Diagnostik des Echinokokkose*, *Fortschr. Röntgenstr.* 133: 164-170 (1980).
9. Itai, Y., Nishikawa, J. and Tabaka, A., *Computed Tomography in Evaluation of Hepatocellular Carcinoma*, *Radiology*, 131: 165-170 (1979).
10. Lassègue, A., Deschamps, J.P., Vuitton, D., Allemand, H., Singer, P., Ottignon, Y., Rohmer, P., Bihr, E., Veillon, F., Belloir, A., Perriguet, G., Carayon, P. and Miguet, J.P., *Apport de la Tomodensitométrie au Diagnostic et à la Surveillance de l'Echinococcose Alvéolaire Hépatique*, *Gastroentérol. Chir. Biol.* 6: 901-909 (1982).
11. Lee, J.K.T., Sagel, S.S. and Stanley, R.J., *Computed Body Tomography*, Raven Press, New York, (1983).
12. Roche, G., Canton, P., Gerard, A., Colin, D., Boissel, P., Chaulieu, C. and Dureux, J.B., *Essai de Traitement de l'Echinococcose Alvéolaire par le Flubendazole*. A propos de 7 Observations, *Med. Mal. Inf.* 12: 218-230 (1982).
13. Schulze, K., Hubener, K.H., Klott, K., Jenss, H. and Bahr, R., *Computer Tomographische Diagnostik der Echinokokkose*, *Fortschr. Röntgenstr.* 132: 514-521, (1980).
14. Scatarige, J.C., Fischman, E.K., Saksouk, F.S. and Siegelman, S.S., *Computed Tomography of Calcified Liver Masses*, *J.Comput.Assist.Tomogr.* 7: 83-89 (1983).
15. Scherer, U., Weinzierl, M., Sturm, R., Schildberg, F.W., Zrenner, M. and Lissner, J., *Computed Tomography in Hydatid Disease of the Liver: a report on 13 cases*, *J. Comput. Assist. Tomogr.* 2: 612-617 (1978).
16. Vasile, N., Kadiri, R., Larde, D., Belloir, C., and Silvera, L., *Séméiologie Tomodensitométrique des Lésions Circonscrites du Foie*, *J. Radiol.* 62: 489-495 (1981).
17. Weill, F., Kraehenbuhl, J.R., Bourgoin, A., Miguet, J.P. and Gillet, M., *Aspects Echotomographiques de l'Echinococcose Alvéolaire*, *Med. Chir. Dig.* 4: 35-37 (1975).
18. Weill, F.S., Le Mouel, A., Bihr, E., Rohmer, P., Zeltner, F. and Perriguet, G., *Ultrasonic Patterns of Acquired Budd-Chiari's Syndromes*, *Europ. J. Radiol.* 1: 236-237 (1982).